Clay Column Chromatography for Optical Resolution: Separation and Asymmetric Induction of Cyclometalated Iridium(III) Complexes

Akihiko Yamagishi,[1*] Kazuyoshi Takimoto,[2] Kyaw Naing,[3] Kenji Tamura,[4] Masumi Kamon[4], Jun Yoshida[5] and Hisako Sato[6*]

[1] Faculty of Medicine, Toho University, Tokyo 143-8540, Japan

[2] Department of Chemistry, School of Science, Kitasato University, Kanagawa 252-0373, Japan

[3] SML College, Yangon 11201, Myanmar

[4] Research Center for Electronic and Optical Materials, National Institute of Materials Science, Tsukuba 305-0044, Japan

[5] Department of Chemistry, College of Humanities & Sciences, Nihon University, Tokyo 156-8550, Japan

[6] Faculty of Science, Ehime University, Ehime 790-8577, Japan

*Corresponding author: Ehime University, Faculty of Science, Ehime 790-8577, Japan

. Email: sato.hisako.yq@ehime-u.ac.jp

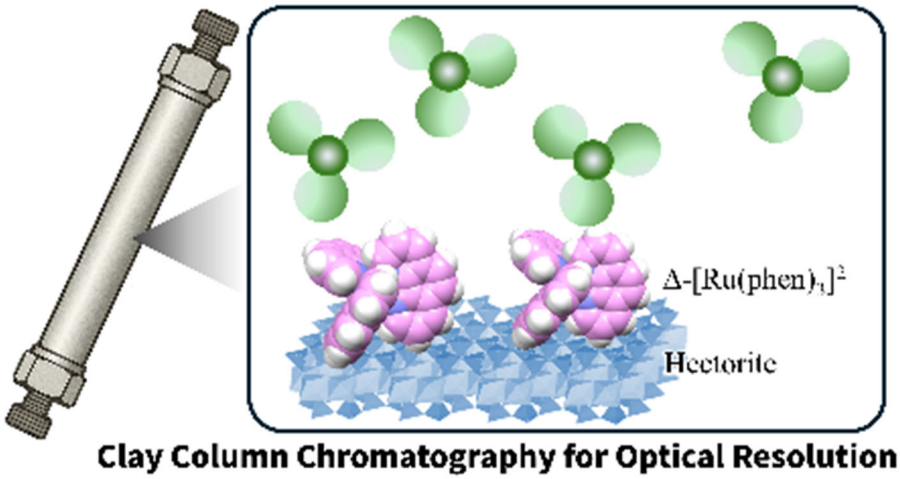
Abstract

Chromatographic separation was attempted by eluting the Ir(III) complexes on a high-performance liquid chromatography (HPLC) column packed with an ion-exchange adduct of synthetic hectorite and 1,10-phenanthroline-Ru(II). The affinity of the stationary phase was adjusted by altering the loading of Δ-$[Ru(phen)_3]^{2+}$ in the hectorite. Seven kinds of neutral iridium(III) complexes were resolved, with two peaks assigned to the Δ- and Λ- enantiomers. The elution order was determined from electronic circular dichroism (ECD) spectra of the more and less retained fractions. Three kinds of positively charged iridium(III) complexes were eluted, yielding Δ-enantiomers with optical purities of 60%–72% as less strongly adsorbed isomers. The opposite enantiomers were too firmly adsorbed for elution. When a five-coordinated iridium(III) complex (*trans*-$[Ir(^{i}PrBQ)_2Cl]$) (^{i}PrBQ = mono-deprotonated 2-isopropylbenzo[*h*]quinoline), was injected, the entire complex was adsorbed and could not be eluted. Adding a negatively charged chelating ligand (disodium salt of 4,7-diphenylphenanthroline disulfate, Na_2BPS) eluted a negatively charged six-coordinated complex (*trans*-$[Ir(^{i}PrBQ)_2BPS]$). Notably, the transformation from Δ- or Λ-*trans*-$[Ir(^{i}PrBQ)_2Cl]$ to *trans*-

[Ir(^{i}PrBQ)$_2$BPS]$^-$ occurred stereoselectively. The eluted complex exclusively took the Δ-conformation from their ECD spectra. This is the first example of the stereoselective transformation of a coordinatively robust Ir (III) complex by passing it through a short column of 1 cm in length. The column uniquely afforded enantiomerically neutral, positively charged, and negatively charged iridium(III) complexes.

Keywords: five-coordinated iridium(III) complexes, stereoselective transformation, vibrational circular dichroism spectroscopy

Graphical Abstract



1. Introduction

Stereoisomers have a wide range of applications in various fields covering synthetic chemistry, biochemistry, medical, clinical, pharmaceutical, and agricultural sciences.[1] Researchers have focused on enantiomeric separations using various techniques such as chromatography, electrophoresis, liquid extraction, and membranes.[2] Among the techniques, the high-performance liquid chromatography (HPLC) using chiral stationary phases (CSPs) is one of powerful tools for obtaining the enantiomers of chiral compounds.[3] Some examples of CSPs are chiral metal coordination complex adducts or polysaccharides (cellulose, amylose, cyclodextrin) and chiral amino acid derivatives. Various types of CSPs have been developed, contributing to better separation, higher selectivity and sensitivity, and sufficient compactness of the columns.[3-10]

We were interested in chiral clay adducts as CSPs for HPLC.[11-14] In our attempts, a chiral metal complex was ion-exchanged as a modifier. A uniform two-dimensional distribution of chiral adsorption sites is observed on the surface of the phyllosilicate layer. The prepared ion-exchange adducts were packed into an HPLC column for enantiomer separation. When a racemic mixture passes through the column, the chiral clay-chelate adduct interacts differently with opposite enantiomers of the molecules, leading to enantiomer resolution.

In the synthetic field of metal complexes, cyclometalated iridium(III) complexes are attracting an extensive attention because of their highly emissive properties in the UV-visible region.[15] They maintain a stable structure at high temperature (> 100 °C) and are resistant to the attack of oxygen molecules. Molecular devices are manipulated based on iridium(III) complexes, such as photosensing, electronic photodevices, emissive medical diagnosis, and photo-catalysts.[16-18]

Chirality played a valuable role in our study. For example, in energy transfer among metal complexes, an ultrathin film of chiral iridium(III) complexes and an exfoliated clay layer were manipulated. [19] The effects of molecular chirality are also an interesting target when a chiral donor/acceptor pair is used in triplet-triplet annihilation for up-conversion (TTA-UC).[19] TTA-UC is applied to realize the amplification of CPL (circularly polarized luminescence) using a chiral acceptor. In the field of biosensing, chiral forms of emissive iridium(III) complexes are promising for detecting anomalies in biological tissues.[20]

Enantiomerically pure isomers of iridium(III) complexes are obtained widely on commercial columns of polysaccharide derivatives (e.g., the Daicel CHIRALPAK IA columns).[19] Practically an appropriate column is selected depending on the charge type of the iridium(III) complex.[21] In our previously reported works, the wide scope of iridium (III) complexes was resolved on polysaccharide derivative-based CSP's.[22-26]

This paper reports an attempt to separate chiral iridium(III) complexes into enantiomers using a

modified clay column. The column was stable for a long period over a wide range of temperature.[11-15] As an attempt, the affinity was adjusted by changing the loading of the chiral modifier. The elution behaviors of the neutral and positively charged iridium(III) complexes were investigated by adjusting the loading of the chiral modifier and the column length.

2. Experimental

Reagents: The iridium(III) complexes used in this study are tabulated in Chart S1 of the Supporting Information. The complexes were synthesized by our group as emitting components in molecular devices such as oxygen sensing, dual emission, chemically polarized emission (CPL), and up-conversion of photon energy.[19-26] Their syntheses and identification are described in the Supporting Information. Synthetic hectorite (Laponite RD, denoted as Na-HEC) was purchased from BYK Additives Instruments (U. K.). Its elemental composition and CEC (cation-exchange capacity) are stated to be $(Na_{0.37}Ca_{0.01})[(Mg_{2.80}Li_{0.19})(Si_{3.96}O_{10})(OH)_2]$ and 0.65 milli-equivalents per gram, respectively. [14] An eluting solvent was a mixture of HPLC-grade methanol/dichloromethane or acetonitrile (HPLC grade). 4-Phenylpyridine (ppyH), $[Ir(dfppy)_2Cl]_2$ (dfppyH = 2-(2', 4'-difluorophenyl)pyridine), $[Ir(piq)_2Cl]_2$ (piqH = 1-phenylisoquinoline) and disodium 4, 7-diphenylphenanthrolinedisulphate (Na_2BPS) were purchased from Kanto Chemical Ind. Co. (Japan). [Ir(dfppy)$_2$(ppy)] and [Ir(piq)$_2$(ppy)] were synthesized according to previously reported methods. [28-31]

Preparation of chiral clay columns: Δ-$[Ru(phen)_3]Cl_2$ was obtained using potassium antimonyl (+)-tartrate as a resolving reagent.[32,33] Spherical particles of Na-HEC were prepared by the spray-dried method as described previously.[13] For preparing a column of 100% loading in terms of cation-exchange capacity, 3.0 g of the spherical particles of Na-HEC was dispersed in 50 mL of methanol. 2.0 g of Δ-$[Ru(phen)_3]Cl_2$ (5×10^{-5} mol) was added slowly under stirring. The clay particle was colored orange, indicating that Δ-$[Ru(phen)_3]^{2+}$ was ion-exchanged with Na^+ ions in Na-HEC spontaneously. The resultant material was denoted as Δ-$[Ru(phen)_3]^{2+}$/HEC (100 % loading). The adsorbed amount of Δ-$[Ru(phen)_3]^{2+}$ was varied from 2% to 100% in terms of the cation-exchange capacity (CEC) of HEC. After filtering the suspension, the solid precipitate or Δ-$[Ru(phen)_3]^{2+}$/HEC was dried under air and packed into a stainless tube of different lengths (1−10 cm × 4 mm (i.d.)). The column temperature was maintained by circulating the water set at each temperature.

Instruments: UV-vis spectra were measured using a U-2810 spectrometer (Hitachi Ind. Co., Japan). Electronic circular dichroism spectra were measured using a polarimeter J-500 (JASCO, Japan). The

emission spectra were recorded using an RF-5300 fluorometer (Shimadzu Co., Japan). High performance liquid chromatography (HPLC) was performed with a PU-980 pump equipped with a UV-975 detector (JASCO, Japan). High-resolution electrospray ionization mass (HR-ESI-MS) spectra were obtained using an Exactive Plus Orbitrap Mass Spectrometer **(**Thermo Fisher Scientific, USA**).**

Preparation and measurements of VCD (Vibrational circular dichroism) samples: An ion-exchange adduct of sodium montmorillonite (Na-Mt) with Δ-Ru(phen)$_3$]$^{2+}$ (denoted as Δ-[Ru(phen)$_3$]$^{2+}$/Mt) was prepared as described previously.[13] An iridium(III) complex (ca. 1 × 10^{-5} mol) was added to 1:1 (v/v) water/methanol (10 mL) dispersing **Δ**-*cis*-[Ir(bzq)$_2$(PBO)]/Δ-[Ru(phen)$_3$]$^{2+}$/Mt or Λ-*cis*-[Ir(bzq)$_2$(PBO)]/Δ-[Ru(phen)$_3$]$^{2+}$/Mt (100 mg or 1×10^{-4} mol of [Ru(phen)$_3$]$^{2+}$). After centrifuging the dispersion, the residue was freeze-dried and mixed with dry KBr powder to a weight percentage of approximately 2%. The material was made into a pellet and used for the VCD measurements.

The VCD spectra were measured using a machine developed in-house with the cooperation of JASCO Corporation, Japan (MultiD-MIRAI-2020 spectrometer). The machine was a concurrent system combined with a quantum cascade laser (QCL-VCD) covering the wavenumber range of 1500–1740 cm^{-1}) and an FT-VCD covering 800–2000 cm^{-1}.[34,35] In this study, the samples were measured in the FT-VCD mode, using a normal cell holder under normal positioning. The wavenumber resolution was 4 cm^{-1}. Signals were accumulated more than 10000 times. No baseline correction was performed for any of the samples.

Computational details: The IR and VCD spectra of the complexes were theoretically calculated using the Gaussian 16 program (C.01).[36] Geometry optimization was performed at the DFT level, in which the B3LYP functional with Stuttgart ECP was employed for Ru(II) and 6-31G(d, p) for the other atoms. In the case for a molecular associate consisting of a derivatized amino acid ester and a metal complex, geometry optimization was performed at the DFT-D3 level. The intensity of the VCD peak is given by the rotational strength, which is the dot product of the electric and magnetic dipole transition moments. The calculated intensities were converted to Lorentzian bands with a half-width of 4 cm^{-1} half-width at half-height. The observed spectra were assigned based on animations of the molecular vibration with Gaussview 6.0 (Gaussian Inc.).

3. Results and discussion

Loading effects of a chiral modifier on the affinity and selectivity toward a targeted iridium(III) complex: The complexes investigated in the current study are tabulated in Chart S1 of the Supporting Information. They possessed planar aromatic ligands and were anticipated to interact strongly with a

chiral modifier (Δ-$[Ru(phen)_3]^{2+}$) in Δ-$[Ru(phen)_3]^{2+}$/HEC through π–π interactions.

Batch experiments were performed to determine the optimum $[Ru(phen)_3]^{2+}$ loading for chiral discrimination. For the purposes, an iridium complex, *cis*-$[Ir(bzq)_2(PBO)]$ (Chart 1), was used since their enantiomers were available in a pure form.[23] Δ- or Λ-isomer of *cis*-$[Ir(bzq)_2(PBO)]$ was mixed with a solid adsorbent (or Δ-$[Ru(phen)_3]^{2+}$/HEC) dispersed in 1:1 (v/v) methanol/dichloromethane. The loading of Δ-$[Ru(phen)_3]^{2+}$ varied from 5% to 100% of the cation-exchange capacity of HEC. Figures 1 A and B show the dependence of the adsorption and selectivity of the investigated complex on loading, respectively. The adsorbed amount of Δ- or Λ-enantiomer was expressed as A_Δ or A_Λ (0%−100%), respectively, in terms of the fraction of the added amount. The stereoselectivity in adsorption is expressed as the ratio of A_Δ/A_Λ. According to the figures, the adsorbed amounts increased with increasing loading, whereas a significant difference was observed in the adsorption between the opposite enantiomers. As a result, A_Δ/A_Λ took the maximum value around 20% loading.

Therefore, the Δ-enantiomer has a more preferential access to adsorption on the solid adsorbent than the Λ-enantiomer. This is owing to the difference in stereoselective interactions between Δ- or Λ-enantiomers with the solid adsorbent. The proper column material for resolving the complex was chosen to be Δ-$[Ru(phen)_3]^{2+}$/HEC at 25% loading.

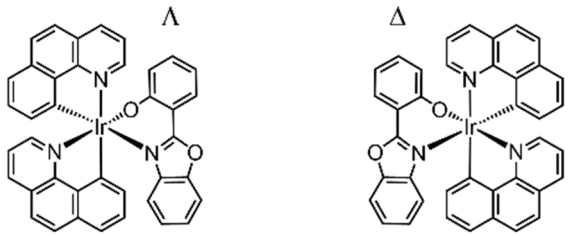


Chart 1. *cis*-$[Ir(bzq)_2(PBO)]$ (bzqH = benzo[*h*]quinoline; PBOH = 2-(2-hydroxylphenyl)benzoxazole)

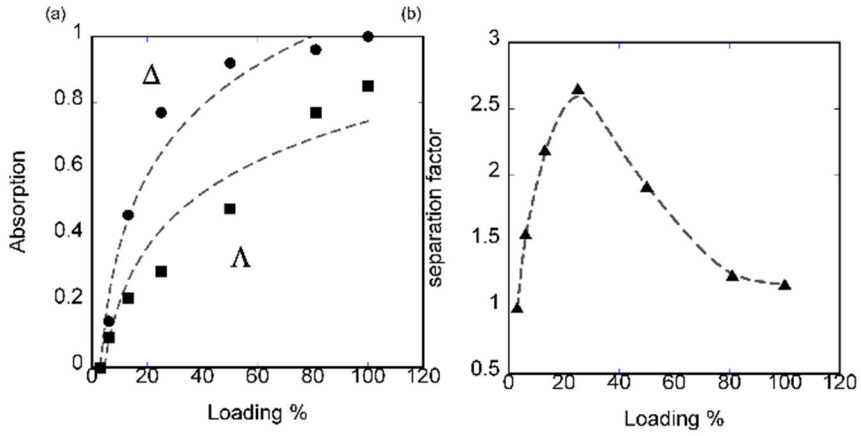


Figure 1. (a) Dependences of adsorption and (b) selectivity of the enantiomers of *cis*-[Ir(bzq)$_2$(PBO)] on the loading of Δ-[Ru(phen)$_3$]$^{2+}$ in Δ-[Ru(phen)$_3$]$^{2+}$/HEC**.** In the experiments, 10 mg of **Δ-**[Ru(phen)$_3$]$^{2+}$/HEC was dispersed in a 0.5 mL of methanol. 5 × 10^{-8} mole of *cis*-[Ir(bzq)$_2$(PBO)] was added to the dispersion. After being left for 1 h, the dispersion was centrifuged. The electronic spectra of filtrates were measured to determine the amounts of free and bound complexes. Selectivity was expressed in terms of the ratios of bound complexes, or A_Δ/A_Λ.

Elution of neutral iridium(III) complexes: cis-[Ir(bzq)$_2$(PBO)], were eluted on a column packed with-[Ru(phen)$_3$]$^{2+}$/HEC. The loading of Δ-[Ru(phen)$_3$]$^{2+}$ was 25% in terms of CEC. Figure 2 shows the chromatogram when a 1:1 mixture of Δ- and Λ-enantiomers of cis-[Ir(bzq)$_2$(PBO)] were eluted at 1.5 °C. Two peaks are observed near the baseline separation. The separation factor is given by

$$\alpha = (V_2\text{-}V_d)/(V_1\text{-}V_d),$$

where V_1, V_2 and V_d are the elution volumes of the fewer and more retained peaks, and the dead volume (0.45 mL), respectively. The value of α was calculated to be 5.2, The results were compared to the separation by the commercially available columns such as SUMICHIRAL OA-3200R (25 cm × 4.6 mm(i.d.)) (Sumika Chemical Analytical Service, Ltd. Japan).[19] The separation efficiency (*f*) is given by:

$$f = (V_2\text{-}V_1)/\{(\text{half width of peak 1}) + (\text{half width of peak 2})\}.$$

The value of *f* was 1.45. Notably, the current column achieved high efficiency despite its short length (10 cm) with no additives in the eluent.

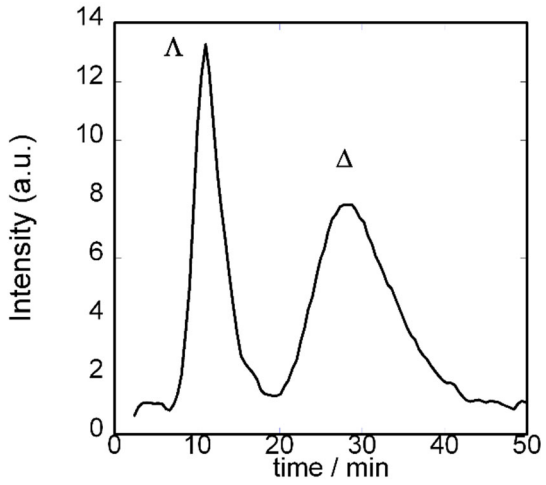


Figure 2. HPLC chromatogram of a 1:1 mixture of Δ- and Λ-enantiomers of *cis*-[Ir(bzq)$_2$(PBO)], when it was eluted on a column (10 cm × 4 mm (i.d.)) packed with Δ-[Ru(phen)$_3$]$^{2+}$/HEC (25% loading)**.** An eluting solvent was 2:1 (v/v) methanol/dichloromethane and an elution rate 0.1 mLmin^{-1}. Monitoring wavelength was 290 nm and temperature 1.5 ℃. From the results of eluting each enantiomer separately under the identical conditions, the first and second peaks were assigned to the Λ- and Δ-enantiomers, respectively. This observation was consistent with the loading effect (Fig. 1A). Owing to the strong preference of the solid adsorbent for the Δ-enantiomer, the Λ-enantiomer is first eluted from the column.

Elution conditions (temperature, solvent composition, and flow rate) were varied. The results are shown in Table S1. information. The separation efficiency was significantly influenced by the flow rate, solvent composition, and temperature. According to the table, the separation efficiency decreased with increasing flow rate (e.g., a (*f*) = 1.7 (0.60), 1.4 (0.50) and 1.3 (0.45) at 0.1, 1.4 and 1.3 mLmin^{-1}). This implied that the adsorption equilibrium took longer than the elution period (~ 10 min). Adsorption sites are present in the interlayer spaces of the clay minerals. A longer time is required for a complex molecule to penetrate the narrow gallery of interlayer spaces. From the effects of temperature, the enthalpy of adsorption was calculated to be -11 or -71 kJmol^{-1} for Δ- or Λ-*cis*-[Ir(bzq)$_2$(PBO)], respectively. The selectivity (or 60 kJmol^{-1} in terms of adsorption energy) arose mainly from the p-p interaction between *cis*-[Ir(bzq)$_2$(PBO)] and Δ-[Ru(phen)$_3$]$^{2+}$. The theoretical simulation results of the interactions between these two molecules are presented in a later section.

The remaining neutral Ir (III) complexes were eluted. They were used as an emitting component in the functional molecular devices developed in our group.[22-27] Choosing the optimum loading and column length, they were resolved with two peaks (or a shoulder) assigned to Δ- or Λ-enantiomers. Here, the absolute configuration of the eluted enantiomer was determined from electronic circular

dichroism (ECD) spectra. The results are summarized in Table 1. This table includes the separation factor (α) and separation efficiency (*f*). Examples of chromatograms and ECD spectra of the collected fractions are shown in the Supporting Information.

Table 1. Resolution of neutral iridium(III) complexes

Compound	Column Loading (length)	V_1/mL	V_2/mL	a	*f*	Elution Order
cis-[Ir(bzq)$_2$(PBO)] **(#1)**	25 % loading (10 cm)	0.42	2.22	5.2	1.45	Λ → Δ
trans-[Ir(ppy)$_2$(PBO)] **(#2)**	25 % loading (10 cm)	0.28	0.56	2.0	0.71	Λ → Δ
fac-[Ir(ppy)$_3$] **(#3)**	25 % loading (5 cm)	0.37	0.77	2.1	0.33	Λ→ Δ
fac-[Ir(dfppy)$_2$(ppy)] **(#4)**	2 % loading (1 cm)	0.11	0.80	7.2	0.33	Δ → Λ
fac-[Ir(piq)$_2$(ppy)] **(#5)**	2 % loading (1 cm)	0.10	0.26	2.6	0.33	Δ→ Λ
trans-[Ir(^{i}PrBQ)$_2$(dbm)] **(#6)**	100 % loading (5 cm)	0.20	0.76	3.8	0.70	Δ → Λ
trans-[Ir(^{i}PrBQ)$_2$(heptacac)] **(#7)**	100 % loading (5 cm)	0.06	0.09	1.5	0.70	Λ → Δ

*) Temperature: 1.5 ~ 12°C, **) Eluting solvent: 5/1 ~ 2/1 (v/v) methanol/dichloromethane

Theoretical studies on interactions between [Ir(bzq)$_2$(PBO)] and Δ-[Ru(phen)$_3$]$^{2+}$: The intermolecular interaction between *cis*-[Ir(bzq)$_2$(PBO)] and enantiomeric [Ru(phen)$_3$]$^{2+}$ was studied theoretically. As a model system, molecular dynamic calculation was performed for a pair of either Δ-*cis*-[Ir(bzq)$_2$(PBO)]/Δ-[Ru(phen)$_3$]$^{2+}$ or Λ-*cis*-[Ir(bzq)$_2$(PBO)]/Δ-[Ru(phen)$_3$]$^{2+}$. According to the elution order of the experimental chromatogram, the former and latter pairs correspond to strongly and weakly interacting pairs, respectively. The simulation began from a state in which the two components were placed apart with no intermolecular interactions. Clay sheets are not included. Instead, one SO_4^{2-} ion was included for charge neutrality. Figures 3 (a) and (b) show the optimized structures. In both the cases, the pair attained an energetically stable structure. According to the association models, the main interaction arises from the stacking interactions of the two planar ligands, bzq$^-$ and phen. Although the distance between two central ions differed between two pairs (0.755 nm for Δ-Ir/Δ-Ru and 0.718 nm for Λ-Ir/Δ-Ru, respectively), the association energy was predicted to be nearly equal for two pairs. This implied that the observed stereoselectivity was achieved not only by enthalpy but also by entropy.

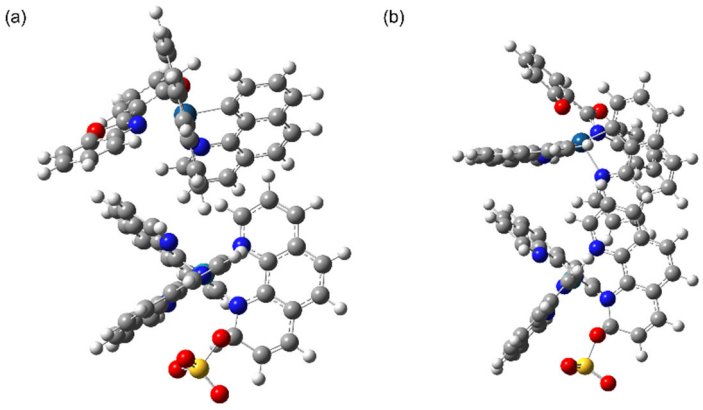


Figure 3. Optimized association structures of (a) Λ-*cis*-[Ir(bzq)$_2$(PBO)]/Δ-[Ru(phen)$_3$]$^{2+}$ and (b) Δ-*cis*-[Ir(bzq)$_2$(PBO)]/Δ-[Ru(phen)$_3$]$^{2+}$.

VCD spectra of clay samples containing enantiomeric cis-[Ir(bzq)$_2$(PBO)] and Δ-[Ru(phen)$_3$]$^{2+}$: VCD spectra were recorded on the samples as described in the experimental section. In case of a montmorillonite sample containing either Δ-or Λ-[Ru(phen)$_3$]$^{2+}$/Mt, the clear peaks assigned to these complexes were observed, maintaining the mirror image relation between the opposite enantiomers as shown in the supporting information. When the montmorillonite contained a pair of Λ-*cis*-[Ir(bzq)$_2$(PBO)] or Δ-*cis*-[Ir(bzq)$_2$(PBO)]/Δ-[Ru(phen)$_3$]$^{2+}$/Mt, the peaks assigned to Δ-[Ru(phen)$_3$]$^{2+}$ retained to be observed in the supporting information. Additionally, there appeared broad peaks in the range of 1300−1400 cm^{-1} and weak mirror-imaged peak of around 1700 cm^{-1}. These were assigned to the bending vibrations of the intercalated PBO$^-$ (Supporting Information). Notably the band was more eminent for Λ-*cis*-[Ir(bzq)$_2$(PBO)]/Δ-[Ru(phen)$_3$]$^{2+}$/Mt than for Δ-*cis*-[Ir(bzq)$_2$(PBO)]/Δ-[Ru(phen)$_3$]$^{2+}$/Mt. The broadening of a VCD peak of an intercalated molecule might be caused by the situations that it took a number of different conformations within a clay mineral.

Elution of positively charged iridium(III) complexes: Positively charged iridium(III) complexes (e.g., compounds # 8–10 in Chart S1) were used as the emitting components in the ultrathin films. They are hybridized with layered clay minerals to form thin films or colloidal particles.[23, 27] The chirality of these molecules plays an important role when the films or particles function as photosensors. The enantiomers were obtained by HPLC resolution on a commercial column.[23] With a purpose of developing another method, an attempt was made to obtain the enantiomers of these compounds using the developed clay column. The preliminary results based on the batch method were reported previously in case of Ir(ppy)$_2$(dmbpy)]PF$_6$ ((ppyH = 2-phenylpyridine, dmbpy = 4,4'-

dimethylbipyridine) (compound # 10 in Chart S1).[27]

A racemic mixture of [Ir(dfppy)$_2$(dmbpy)]PF$_6$ (dmbpy = 4,4'-dimethylbipyridine) (compound # 8 in Chart S1) was eluted on Δ-[Ru(phen)$_3$]$^{2+}$/HEC with 100% loading. Despite the short column (1 cm in length), the mounted complex eluted slowly for an hour. The eluted solution was collected and analyzed using ECD. The solution contained the Δ-enantiomer as an excess enantiomer. The optical purity was 60% by using a commercial column (Supporting Information). The remaining mounted complex was adsorbed too tightly to be eluted with flowing dichloromethane over several hours. The same experiments were performed for Ir(piq)$_2$(dmbpy)]PF$_6$, Ir(ppy)$_2$(dmbpy)]PF$_6$ and (complexes # 9 and # 10, as shown in Chart S1, respectively). For these complexes, their Δ-enantiomers were eluted at the optical purity of 60%−72 %. Notably, if the same experiment was performed on a column of Λ-[Ru(phen)$_3$]$^{2+}$/HEC, Λ-enantiomers would be obtained. The results are summarized in Table 2.

Table 2. Elution of three kinds of positively charged racemic iridium(III) complexes on a column of Δ-[Ru(phen)$_3$]$^{2+}$ /HEC (100% loading and 1 cm in length). For elution, methanol was flowed at a flow rate of 1 mL/min for 30 min.

Complex	Eluted enantiomer	Optical purity (%)
[Ir(dfppy)$_2$dmbpy]$^+$	Δ	72 ± 5
[Ir(piq)$_2$dmbpy]$^+$	Δ	60 ± 5
[Ir(ppy)$_2$dmbpy]$^+$	Δ	60 ± 5

* Column: Δ-[Ru(phen)$_3$]$^{2+}$/HEC (100% loading, 1cm in length) ** Eluent: Methanol

Elution of five-coordinated iridium(III) complexes: Most of the reported stable cyclometalated iridium(III) complexes adopt an octahedral six-coordinate structure. Recently, several five-coordinated iridium(III) complexes, distinct from the conventional six-coordinated ones, have been reported.[37–40] Their enantiomers were obtained on a commercially available chiral column and revealed that they serve as chiral intermediates to afford six-coordinated complexes under mild conditions.[25] Moreover, these complexes exhibit enantioselective supramolecular assembly behaviors as well as thermochromism and mechanochromism.[26]

For studying the elution behavior of a five-coordinated iridium(III) complex, the Δ- or Λ-enantiomer of [Ir(^{i}PrBQ)$_2$Cl] (^{i}PrBQ = mono-deprotonated 2-isopropylbenzo[*h*]quinoline (Chart 2) was injected. Since the complex showed extremely high affinity towards Δ-[Ru(phen)$_3$]$^{2+}$ /HEC, a column (100 % loading, 1cm in length) was used. The surface was covered fully with Δ-[Ru(phen)$_3$]$^{2+}$ ions to avoid the interaction between [Ir(^{i}PrBQ)$_2$Cl] and a bare surface.

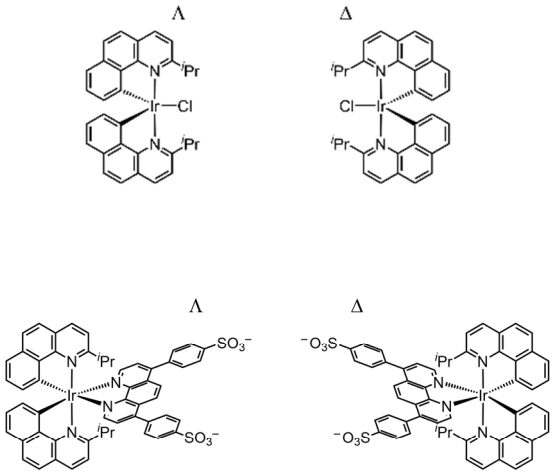


Chart 2. [Ir(^{i}PrBQ)$_2$Cl] (^{i}PrBQ = monodeprotonated 2-isopropylbenzo[*h*]quinoline) (top) and [Ir(^{i}PrBQ)$_2$(BPS)]$^-$ (Na_2BPS = disodium salt of 4, 7-diphenylphenanthroline disulfonic acid) (bottom).

No elution occurred when 1:1 (v/v) methanol/dichloromethane was passed through the column for 30 min after the injection of [Ir(^{i}PrBQ)$_2$Cl]. To recover the injected complex from the column, a negatively charged ligand, 4, 6-diphenylphenanthrolinedisulfonic disodium (Na_2BPS), was injected and passed through methanol. A slightly reddish complex was eluted slowly in 1 h. When the electronic spectrum of the collected fraction was measured, it was identical to that of [Ir(^{i}PrBQ)$_2$BPS]$^-$, which was separately prepared by adding Na_2BPS to a methanol solution of [Ir(^{i}PrBQ)$_2$Cl] (the supporting information). These results suggest the occurrence of the following reactions within the column:

$$[Ir(^iPrBQ)_2Cl] + Na_2BPS \rightarrow Na[Ir(^iPrBQ)_2BPS] + NaCl. \qquad (1)$$

The ECD spectra of the collected fractions were measured, when the above experiment was performed by injecting either Δ- or Λ-[Ir(^{i}PrBQ)$_2$Cl] initially. Notably, both exhibited nearly identical ECD spectra (Figure 4). They were similar to that of Δ-[Ir(^{i}PrBQ)$_2$BPS]$^-$. The results suggested that the reaction proceeded to produce the Δ-isomer dominantly irrespective of the absolute configuration of an initial five-coordinated complex. The control was achieved evidently through the intermolecular interaction of [Ir(^{i}PrBQ)$_2$Cl] with a chiral modifier, Δ-[Ru(phen)$_3$]$^{2+}$, on a clay surface. The observation was compared with the previously reported example of anti-racemization, or racemic [Ni(phen)$_3$]$^{2+}$ was transformed completely to Λ-[Ni(phen)$_3$]$^{2+}$, when the former was mixed with a methanol dispersion of Δ-[Ru(phen)$_3$]$^{2+}$ /HEC.[41] However, the current finding was more surprising, considering that [Ir(^{i}PrBQ)$_2$Cl] maintained its conformation strictly when it transformed to a six-

coordinated complex in a homogeneous solution. This observation demonstrates the unique aspect of the current column material.

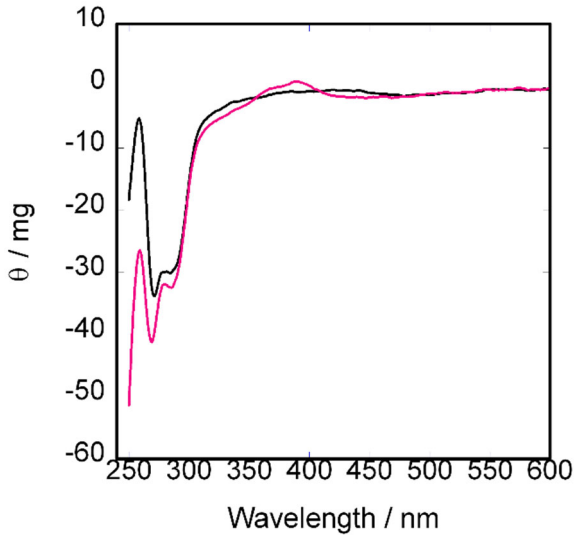


Figure 4. Electronic circular dichroism (ECD) spectra when Δ- or Λ-[Ir(^{i}PrBQ)$_2$Cl] (red or black curves, respectively) was eluted from a column of Δ-[Ru(phen)$_3$]$^{2+}$/HEC on adding Na_2BPS. The reaction started by injecting Δ- or Λ-[Ir(^{i}PrBQ)$_2$Cl] initially.

4. Conclusion

The elution behavior was investigated when cyclometalated iridium(III) complexes were injected on a HPLC (high performance liquid chromatography) column packed with Δ-[Ru(phen)$_3$]$^{2+}$/HEC. The loading of-[Ru(phen)$_3$]$^{2+}$ varied according to the adsorption affinity of the target complex. Consequently, the seven neutral complexes were partially separated into opposite enantiomers. Three positively charged complexes were eluted to give Δ-enantiomers at the optical purity higher than 60%. A five-coordinate iridium(III) complex underwent a stereoselective structural transformation to a six-coordinate complex within the column. These results demonstrate the unique chiral characteristics of the clay surface modified with [Ru(phen)$_3$]$^{2+}$. The unique characteristics of the current column are emphasized in the following points: (i) A single type of column material realized the production of enantiomers of various kinds of iridium(III) complexes covering neutral, positively, and negatively charged species; in particular, even a column of 1 cm in length achieved nearly complete resolution. (ii) The affinity of a stationary phase was varied simply by charging different amounts of a chiral modifier (Δ-[Ru(phen)$_3$]$^{2+}$). (ii) The five-coordinate Ir (III) complex, which was probably chirally robust, underwent stereoselective transformation during elution. This demonstrated

the extremely high steric control of the chiral surface of the present column. However, none of these properties have been realized using conventional chiral columns**.**

Acknowledgement

Thanks are due to Mr. Y. Jinsenji for his synthesis of cis-[Ir(bzq)$_2$(PBO)] and trans-[Ir(ppy)$_2$(PBO)]. This work was financially supported by the Japan Society for the Promotion of Science (JSPS) KAKENHI Grants (JP17H03044, JP20K21090, JP22H02033, JP23K23301, JP23K13766 and JP23K04783). The computations were performed in collaboration with the Research Center for Computational Science, Okazaki, Japan (Project25-IMS-C180).

Supplementary data

Molecular structures of the used iridium(III) complexes; syntheses and identification of iridium(III) complexes; influence of elution conditions on resolving cis-[Ir(bzq)$_2$(PBO)]; chromatograms and electronic circular dichroism spectra of neutral iridium(III) complexes; analyses of optical purity of [Ir(ppy)$_2$(dmbpy)]$^+$ by use of a chiral column; vibrational circular dichroism for cis-[Ir(bzq)$_2$(PBO)]. Supplementary material is available at Bulletin of the Chemical Society of Japan.

Funding

This work was financially supported by the Japan Society for the Promotion of Science (JSPS) KAKENHI Grants (JP17H03044, JP20K21090, JP22H02033, JP23K23301, JP23K13766 and JP23K04783).

Conflict of interest statement.

There are no conflicts to declare.

References

1. W. Guan, W. Zhou, J. Lu, C. Lu, Chem. Soc. Rev. 2015, 44, 56981; S. Aoki, K. Yokoi, Y. Hisamatsu, C. Balachandran, Y. Tamura, T. Tanaka, Top. Curr. Chem., 2022, 380, 36; K. Ariga, R. Fakhrullin, Bull. Chem. Soc. Jpn. 2022, 95, 774.
2. H. Lorenz, A. Seidel-Morgenstern, Angew. *Chem. Int. Ed. 2014, 53, 1218; P. Peluso, B. Chankvetadze, Chem. Rev.* 2022, 122, 13235; J. Sui, N. Wang, J. Wang, X. Huang, T. Wang, L. Zhou, H. Hao, Chem. Sci. 2023, 14, 11955.
3. J. Shen, Y. Okamoto, Chem. Rev. 2016, 116, 1094; K. Tamura, N. S. Md. Sam, T. Ikai, Y. Okamoto, E. Yashima, Bull. Chem. Soc. Jpn. 2011, 84, 741; C. Yamamoto, Y. Okamoto, Bull. Chem. Soc. Jpn.

2004, 77, 227.
4. D. C. Patel, F. Wahab, D. W. Armstrong, A. S. Breitbach, J. Chromatogr. A 2016, 1467, 2.
5. M. F. Wahab, D. C. Patel, R. M. Wimalasinghe, D. W. Armstrong, Anal. Chem. 2017, 89, 8177.
6. H. Liu, Z. Wu, J. Chen, J. Wang, H. Qiu, J. Chromatogr. A 2023, *1708, 464367.*
7. Y. Hong, C. J. Welch, P. Piras, H. Tang, Anal. Chem. 2024, 96, 2351.
8. K. Saigo, Y. Yuki, H. Kimoto, T. Nishida, M. Hasegawa, Bull. Chem. Soc. Jpn. 1988, 61, 322.
9. K. Ariga, A. Vinu, Y. Yamauchi, Q. Ji, J. P. Hill, Bull. Chem. Soc. Jpn. 2012, 85, 1.
10. E. Yashima, Y. Okamoto, Bull. Chem. Soc. Jpn. 1995, 68, 3289.
11. E. Kanao, Y. Murata, S. Miwa, H. Takikawa, K. Takasu, Y. Ishihama, T. Kubo, Anal. Chem. 2025, 97, 12690.
12. A. Yamagishi, M. Taniguchi, Y. Imamura, H. Sato, Appl. Clay Sci. 1996, 11, 1.
13. A. Yamagishi, H. Sato, Clays and Clay Miner. 2012, 60, 411.
14. A. Yamagishi, K. Takimoto, K. Tamura, F. Sato, H. Sato, Bull. Chem. Soc. Jpn. 2021, 94, 2711.
15. A. Yamagishi, S. Yamamoto, K. Takimoto, K. Tamura, M. Kamon, F. Sato, H. Sato, Bull. Chem. Soc. Jpn. 2022, 95, 961. 16. A. Yamagishi, K. Tamura, M. Kamon, J. Yoshida, H. Sato, *Appl. Clay Sci. 2024, 251, 107290.*
17. P. Dey, P. Rai, B. Maji, ACS Org. Inorg. Au 2022, 2, 99.
18. F. Monti, A. Baschieri, L. Sambri, N. Armaroli, Acc. Chem. Res. 2021, 54, 1492.
19. L. C.-C. Lee, K. K.-W. Lo, Chem. Rev. 2024, 124, 8825.
20. A. Yamagishi, K. Takimoto, R. Ito, J. Yoshida, H. Sato, Appl. Clay Sci. 2025, 272, 107828.
21. X. Li, Z. Wang, X. Hao, J. Zhang, X. Zhao, Y. Yao, W. Wei, R. Cai, C. He, C. Duan, Z. Guo, J. Zhao, X. Wang, J. Am. Chem. Soc. 2023, 145, 14766.
22. X. Chen, Y. Okamoto, T. Yano, J. Otsuki, J. Sep. Sci. 2007, 30, 713.
23. H. Sato, K. Tamura, M. Taniguchi, A. Yamagishi, New J. Chem. 2010, 34, 617.
24. K. Tamura, A. Yamagishi, T. Kitazawa, H. Sato, *Phys. Chem. Chem. Phys.* **2015**, 17, 18288.
25. Y. Jinsenji, K. Takimoto, J. Yoshida, S. Mori, Y. Watanabe, H. Sato, *Dalton Trans.* **2021**, *50*, 8506.
26. K. Takimoto, Y. Watanabe, J. Yoshida, H. Sato, *Dalton Trans.* **2021**, *50,* 13256.
27. K. Takimoto, T. Shimada, K. Nagura, J. P. Hill, T. Nakanishi, H. Yuge, S. Ishihara, J. Labuta, H. Sato, *J. Am. Chem. Soc.* **2023***, 145*, 25160.
28. H. Sato, K. Tamura, R. Aoki, M. Kato, A. Yamagishi, *Chem. Lett.* **2011**, *40,* 63.
29. G. Y. Park, J.-H. Seo, Y. K. Kim, Y. S. Kim, Y. Ha, *J. Korean Phys. Soc.* **2007**, *50*, 1729.
30. A. Maity, B. L. Anderson, N. Deligonul, T. G. Gray, *Chem. Sci.* **2013**, *4*, 1175.
31. S. Huo, J. C. Deaton, M. Rajeswaran, W. C. Lenhart, *Inorg. Chem.* **2006**, *45*, 3155.
32. J. C. Deaton, R. H. Young, J. R. Lenhard, M. Rajeswaran, S. Huo, *Inorg. Chem.* **2010**, *49*, 9151.

33. A. Yamagishi, *J. Am. Chem. Soc.* **1985**, *107*, 732.

34. A. Yamagishi, *J. Phys. Chem.* **1984**, *88*, 5709.

35. H. Sakuma, K. Tamura, M. Minagawa, Chem. Lett. 2018, 47, 68.

36. H. Sato, M. Shimizu, K. Watanabe, J. Yoshida, I. Kawamura, J. Koshoubu, Anal. Chem. 2021, 93, 2742.

37. H. Sato, M. Shimizu, K. Watanabe, J. Yoshida, I. Kawamura, J. Koshoubu, Chem. Lett. 2021, 50, 1543.

38. M. J. Frisch, G. W. Trucks, H. B. Schlegel, G. E. Scuseria, M. A. Robb, J. R. Cheeseman, G. Scalmani, V. Barone, G. A. Petersson, H. Nakatsuji, X. Li, M. Caricato, A. V. Marenich, J. Bloino, B. G. Janesko, R. Gomperts, B. Mennucci, H. P. Hratchian, J. V. Ortiz, A. F. Izmaylov, J. L. Sonnenberg, D. Williams-Young, F. Ding, F. Lipparini, F. Egidi, J. Goings, B. Peng, A. Petrone, T. Henderson, D. Ranasinghe, V. G. Zakrzewski, J. Gao, N. Rega, G. Zheng, W. Liang, M. Hada, M. Ehara, K. Toyota, R. Fukuda, J. Hasegawa, M. Ishida, T. Nakajima, Y. Honda, O. Kitao, H. Nakai, T. Vreven, K. Throssell, J. A. Montgomery, Jr., J. E. Peralta, F. Ogliaro, M. J. Bearpark, J. J. Heyd, E. N. Brothers, K. N. Kudin, V. N. Staroverov, T. A. Keith, R. Kobayashi, J. Normand, K. Raghavachari, A. P. Rendell, J. C. Burant, S. S. Iyengar, J. Tomasi, M. Cossi, J. M. Millam, M. Klene, C. Adamo, R. Cammi, J. W. Ochterski, R. L. Martin, K. Morokuma, O. Farkas, J. B. Foresman, D. J. Fox, Gaussian 16 (Revision C.01), Gaussian, Inc. Wallingford, CT, 2019.

39. C. Xu, Z.-Q. Wang, X.-M. Dong, X.-Q. Hao, X.-M. Zhao, B.-M. Ji, M.-P. Song, Inorg. *Chim. Acta 2011, 373, 306.*

40. S. I. Bezzubov, P. Kalle, A. A. Bilyalova, S. V. Tatarin, V. D. Dolzhenko, Chem. Eur. J. 2018, 24, 12779.

41. S. V. Tatarin, S. I. Bezzubov, Inorg. *Chem. 2024, 63, 18642.*

42. E. V. Nykhrikova, M. A. Kiseleva, P. Kalle, S. S. Mariasina, S. A. Kozyukhin, S. V. Tatarin, S. I. Bezzubov, Inorg. Chem. 2025, 64, 5210. 43. H. Sato, K. Takimoto, J. Yoshida, A. Yamagishi, Bull. Chem. Soc. Jpn. 2021, 94, 1.

Supporting Information

Clay Column Chromatography for Optical Resolution: Separation and Asymmetric Induction of Cyclometalated Iridium(III) Complexes

Akihiko Yamagishi,[1] Kazuyoshi Takimoto,[2] Kyaw Naing,[3] Kenji Tamura,[4] Masumi Kamon[4], Jun Yoshida[5] and Hisako Sato[6]*

[1] Faculty of Medicine, Toho University, Tokyo 143-8540, Japan

[2] Department of Chemistry, School of Science, Kitasato University, Kanagawa 252-0373, Japan

[3] SML College, Yangon 11201, Myanmar

[4] Research Center for Electronic and Optical Materials, National Institute of Materials Science, Tsukuba 305-0044, Japan

[5] Department of Chemistry, College of Humanities & Sciences, Nihon University, Tokyo 156-8550, Japan

[6] Faculty of Science, Ehime University, Ehime 790-8577, Japan

Contents

1. Molecular structures of the used iridium(III) complexes

2. Syntheses and identification of iridium(III) complexes

3. Influence of elution conditions on resolving *cis*-[Ir(bzq)$_2$(PBO)]

4. Chromatograms and electronic circular dichroism spectra of neutral Ir(III) complexes

5. Analyses of optical purity of [Ir(ppy)$_2$(dmbpy)]$^+$ by use of a chiral column

6. Vibrational circular dichroism for *cis*-[Ir(bzq)$_2$(PBO)]

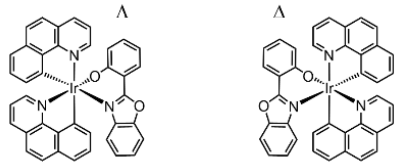
1. Molecular structures of the used iridium(III) complexes

The following chart lists the molecular structures of the iridium(III) complexes used in this work:

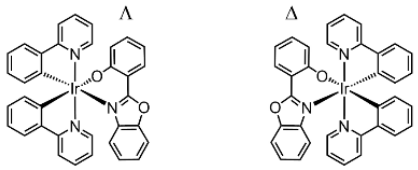
Chart S1. Molecular structures of iridium(III) complexes

Number Compound and molecular structure (remarks)

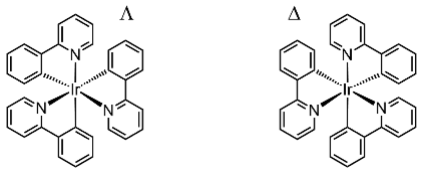
1 *cis*-[Ir(bzq)2(PBO)] (bzqH = benzo[h]quinoline; PBOH = 2- (2-hydroxylphenyl)benzoxazole) (reported in reference (1))



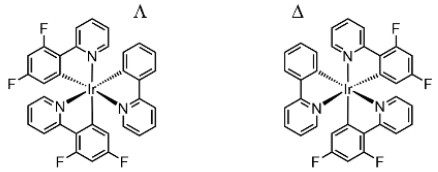
2 *trans*-[Ir(ppy)2(PBO)] (ppyH = 2-phenylpyridine; PBOH = 2- (hydroxylphenyl)benzoxazole) (described later in the supporting information)



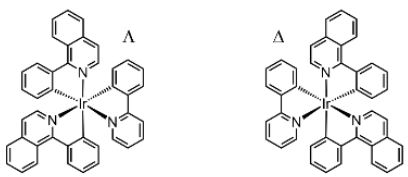
3 *fac*-[Ir(ppy)3] (ppyH = 2-phenylpyridine) (reported in reference (2))



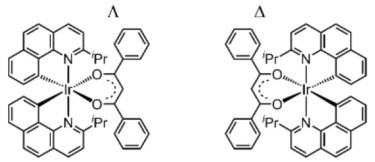
4 *fac*-[Ir(dfppy)2(ppy)] (dfppyH = 2-(2', 4'-difluorophenyl)pyridine); ppyH = 2-phenylpyridine) (described later in the supporting information)



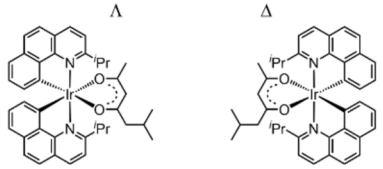
5 *fac*-[Ir(piq)2(ppy)] (piqH = 1-phenylisoquinoline; ppyH = 2-phenylpyridine) (described later in the supporting information)



#6 *trans*-[Ir(iPrBQ)$_2$(dbm)] (iPrBQH = 2-isobutyl-benzo[h]quinolinex; dbmH = dibenzoylmethane) (described later in the supporting information)



#7 *trans*-[Ir(iPrBQ)$_2$(heptacac)] (heptacacH = 6-methyl-2,4-heptadione ($CH_3COCH_2COCH_2CH(CH_3)_2$) (described later in the supporting information)



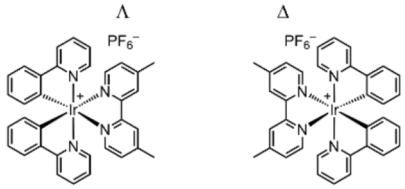
#8 [Ir(dfppy)$_2$(dmbpy)]PF_6 (dmbpy = 4,4'-dimethylbipyridine) (reported in reference (3))



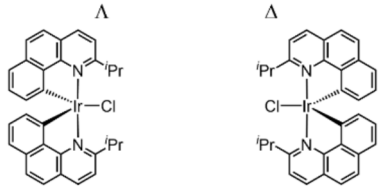
#9 [Ir(piq)$_2$(dmbpy)]PF_6 (reported in reference (3))



#10 [Ir(ppy)$_2$(dmbpy)]PF_6 (reported in reference (4))

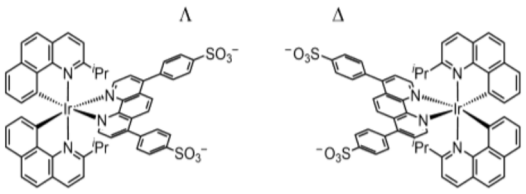


#11 *trans*-[Ir(iPrBQ)2Cl] (iPrBQ=mono-deprotonated 2-isopropylbenzo[*h*]quinoline) (reported in reference (5))



#12 *trans*-[Ir(iPrBQ)2(BPS)]- (Na2BPS = bathophenanthroline disulfonic acid disodium salt)

(described later in the supporting information)



References:

1. Y. Jinsenji, K. Takimoto, J. Yoshida, S. Mori, Y. Watanabe, and H. Sato**,** *Dalton Trans.* **2021**, 50, 8506-8511.
2. H. Sato, K. Tamura, M. Taniguchi and A. Yamagishi, *New J. Chem.* **2010**, *34*, 617.
3. K. Tamura, A. Yamagishi, T. Kitazawa, H. Sato, *Phys. Chem. Chem. Phys.* **2015**, 17, 18288.
4. H. Sato, K. Tamura, R. Aoki, M. Kato, and A. Yamagishi, *Chem. Lett.* **2011**, 40, 63.
5. K. Takimoto, T. Shimada, K. Nagura, J. Hill, T. Nakanishi, H. Yuge, S. Ishihara, J. Labuta, H. Sato, *J. Am. Chem. Soc.***2023**, 145, 25160.

2. Syntheses and identification of the iridium(III) complexes

(i) The syntheses and identification of the following compounds are already described in the literatures: *cis*-[Ir(bzq)$_2$(PBO)] (reference 1), *fac*-[Ir(ppy)$_3$] (reference 2); [Ir(dfppy)$_2$(dmbpy)]PF$_6$ (reference 3); [Ir(ppy)$_2$(dmbpy)]PF$_6$ (reference 4); [Ir(piq)$_2$(dmbpy)]PF$_6$ (reference 3) and *trans*-[Ir(^{i}PrBQ)$_2$Cl] (reference 5). The literatures are numbered in the same way as given in the proceeding section.

(ii) *Trans*-[Ir(ppy)$_2$(PBO)] was synthesized in this work. The procedures were following (reference 1): [Ir(ppy)$_2$Cl]$_2$（100 mg, 0.095 mmol）and Na_2CO_3（72 mg, 0.68 mmol）were dispersed in 1/1 (v/v) 2-ethoxyetanol/water (20 mL). Under stirring in nitrogen atmosphere, 2-(2-hydroxyphenyl)oxazole（51 mg, 0.24 mmol）was added slowly. The mixture was heated at 110°C for 12hours. After cooling, the reactant was mixed with water (100 mL) and filtered. The residue was washed with water, hexane and diethyl ether, successively. The residue was dried in vacuum and recrystallized from 1/1 (v/v) CH_2Cl_2/hexane. According to H1-NMR analyses, the resultant yellow crystal was identified to be *trans*-[Ir(ppy)2(PBO)]（m.w. 698.76, 99.4 mg, 0.142 mmol, yield 75%）. H1-NMR analyses: δH (400 MHz; CDCl3) 6.07 (1H, d, *J* =8.2 Hz), 6.20 (1H, d, *J* =7.5 Hz), 6.47 (2H, m), 6.77 1H, m), 6.82 (1H, d, *J* =7.6 Hz), 6.87 (1H, d, *J* =7.8 Hz), 6.91 (1H, d, *J* =6.1 Hz), 6.94 (1H, d, *J* =7.3 Hz), 7.05 (1H, m), 7.13 (1H, t, *J* =7.8 Hz), 7.19 (1H, td, J = 15.6 and 6.8 Hz), 7.43 (1H, d, *J* =8.0 Hz), 7.57 (1H, d, *J* =7.0 Hz), 7.63 (2H, d, *J* =8.0 Hz), 7.66 (1H, d, *J* =6.8 Hz), 7.79 (1H, d, *J* =8.0 Hz), 7.88 (1H, d, *J* =8.3 Hz), 7.98 (1H, dd, *J* =6.3 and 1.4 Hz), 8.12 (1H, d, *J* =5.6 Hz), 8.87 (1H, d, *J* =5.6 Hz).

(iii) [Ir(dfppy)$_2$(ppy)] and [Ir(piq)$_2$(ppy)] were synthesized in this work. The procedures were following: [{Ir(dfppy)$_2$}$_2$Cl$_2$] (12mg; 1mmole) and ppyH (5 mg; 3.3mole) or [{Ir(piq)$_2$}$_2$Cl$_2$] (13mg, 1mmole) and ppyH (5 mg; 3.3mole) were dispersed in glycerol (20 mL). The mixtures were heated at 190°C for 48 hours. The reactants were cooled and poured into water (100 mL) and extracted with chloroform. After evaporating the chloroform solution to dryness, the residues were injected on a HPLC column (4 mm(i.d.) × 25 cm) (CAPCELL AQ-PAK, Shiseido Co. Ltd., Japan)) and eluted with acetonitrile. The main peaks were collected and proceeded to mass spectroscopic analyses. As shown below, the compounds were identified to be [Ir(dfppy)$_2$(ppy)] ($IrC_{33}H_{23}N_3F_4$; m.w. 726.74) and [Ir(piq)$_2$(ppy)] ($IrC_{41}H_{28}N_3$; m.w. 684.66), respectively.

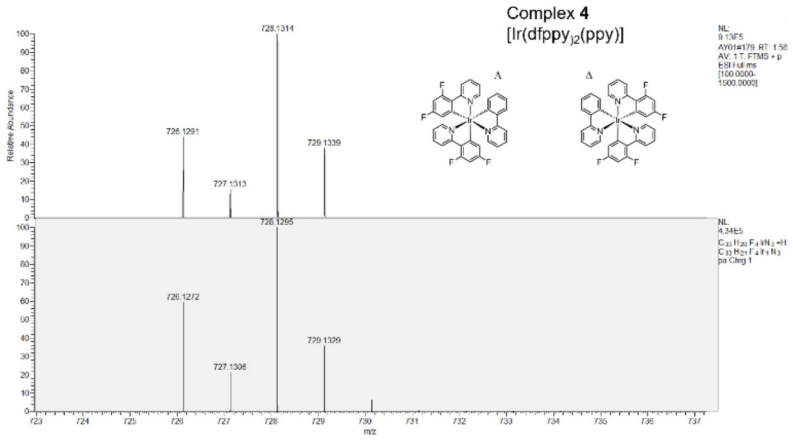


Figure S1. High-resolution ESI mass spectrum of [Ir(dfppy)$_2$(ppy)] measured in acetone, Acetonitrile was introduced as a carrier solvent. The upper panel shows the experimental isotopic pattern centered at m/z 728.1314, and the lower panel the calculated pattern for the protonated molecular ion $[M + H]^+$ of $C_{33}H_{21}F_4IrN_3$ (Calculated: m/z = 728.1295). The observed peak matches well with the theoretical isotopic distribution, confirming the molecular formula.

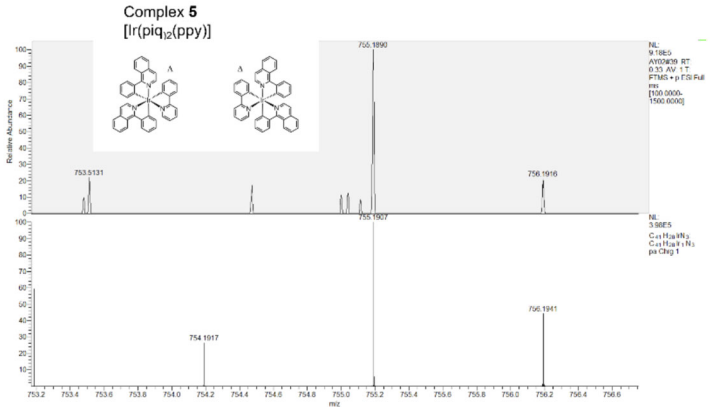


Figure S2. High-resolution ESI mass spectrum of [Ir(piq)$_2$(ppy)] measured in acetone. Acetonitrile was introduced as a carrier solvent. The upper panel shows the experimental isotopic pattern centered at m/z 755.1890, and the lower panel the calculated pattern for the protonated molecular ion [M]+ of C41H28IrN3 (Calculated: m/z = 755.1907). The observed peak matches well with the theoretical isotopic distribution, confirming the molecular formula.

(iv) *Trans*-[Ir(^{i}PrBQ)$_2$(heptacac)], *trans*-[Ir(^{i}PrBQ)$_2$(dbm)] and *trans*-[Ir(^{i}PrBQ)$_2$(BPS)]- were prepared in a solution *in situ* according to the following procedures: A five-coordinated Ir(III) complex (10^{-6} mole), *trans*-[Ir(^{i}PrBQ)$_2$Cl], was dissolved in methanol (10 mL) (denoted as solution **A)**. Free chelating ligands, heptacacH or dbmH and Na_2BPH), were dissolved to c.a. 10^{-6} mole in methanol. They were added to solution **A** in a dropwise way. The formation of a six-coordinated

Ir(III) complex proceeded quantitatively as monitored by the electronic absorption spectra. The example is shown below in case of the formation of *trans*-[Ir(^{i}PrBQ)$_2$(BPS)]$^-$.

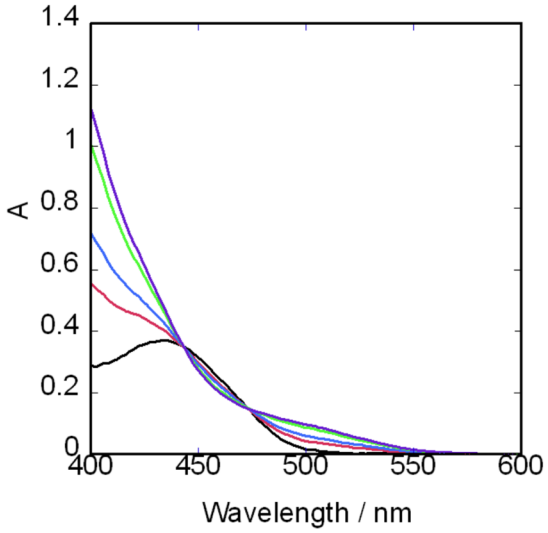


Figure S3. Electronic spectra of the formation of *trans*-[Ir(^{i}PrBQ)$_2$(BPS)]$^-$ on adding Na_2BPS (bathophenanthroline disulfonic acid disodium salt) to a methanol solution of *trans*-[Ir(^{i}PrBQ)$_2$Cl]. The molar ratio of Na_2BPH to *trans*-[Ir(^{i}PrBQ)$_2$Cl] was 0, 0.2, 0.4, 0.6. 0.8 and 1.0 for black, pink, blue, green and deep blue curves, respectively.

3. Influence of elution parameters on separating the enantiomers of *cis*-[Ir(bzq)$_2$(PBO)]

Resolution of *cis*-[Ir(bzq)$_2$(PBO)] was attempted on an HPLC column of Δ-[Ru(phen)$_3$]$^{2+}$/HEC* under various elution conditions. The results are summarized in the following table.

Temperature/°C		Flow rate/mLmin^{-1}	Eluent**	V_1/mL	V_2/mL	α	*f*	elution order
1.5	0.1	2/1(v/v)	MeOH/DCM	0.42	2.22	5.2	1.45	Λ → Δ
14.5	0.1	2/1(v/v)	MeOH/DCM	0.34	0.54	1.5	0.79	Λ → Δ
14.5	0.1	1/2(v/v)	MeOH/DCM	0.13	0.19	1.4	0.50	Λ → Δ
14.5	0.1	1/1(v/v)	MeOH/DCM	0.16	0.28	1.7	0.60	Λ → Δ
14.5	0.2	1/1 (v/v)	MeOH/DCM	0.18	0.23	1.4	0.50	Λ → Δ
14.5	0.5	1/1 (v/v)	MeOH/DCM	0.30	0.40	1.3	0.45	Λ → Δ

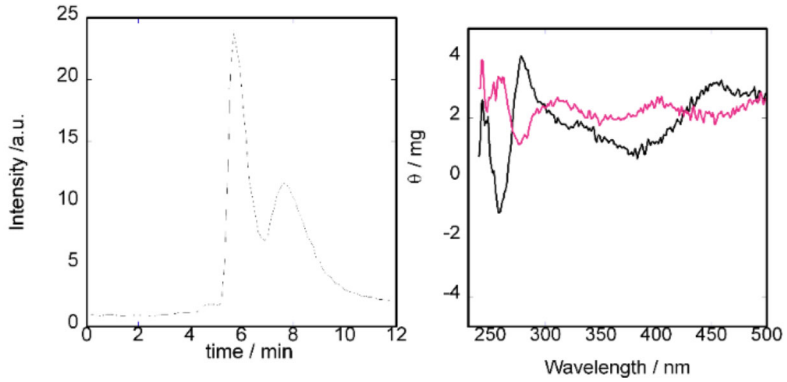
* Column; loading at 25 % and length of 5cm

** MeOH = methanol and DCM = dichloromethane

4. Chromatograms and electronic circular dichroism spectra of the neutral iridium(III) complexes

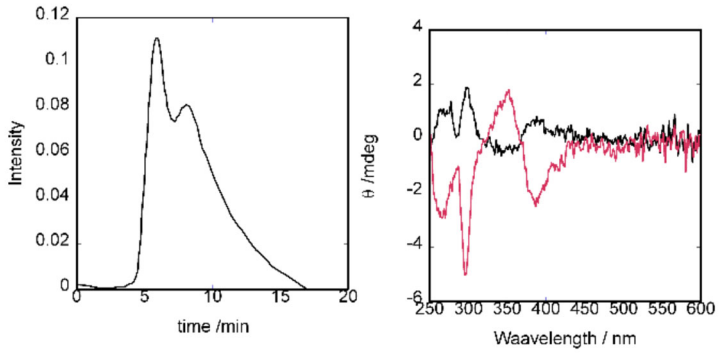
The examples of chromatograms (left) and electronic circular dichroism spectra (right) are shown below for the neutral iridium(III) complexes (Table 1 in the text). The complexes are numbered according to Chart S1. The black and red curves in the ECD spectra are for the less and more retained enantiomers, respectively.

2 : *trans*-[Ir(ppy)$_2$(PBO)]



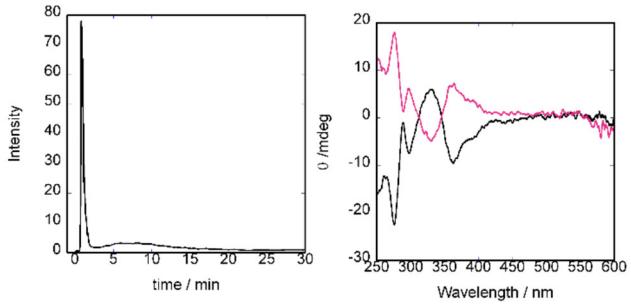
Elution conditions: column (Δ-[Ru(phen)$_3$]$^{2+}$/HEC (10cm, 25%)), eluent (2/1 (v/v) methanol/dichloromethane), flow rate (0.1 mLmin-1), wavelength (290 nm).

#3; *fac*-[Ir(ppy)$_3$]



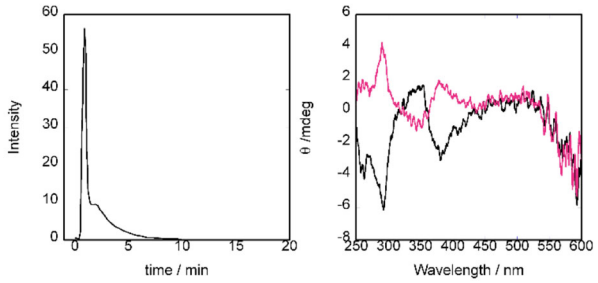
Elution conditions: column (Δ-[Ru(phen)$_3$]$^{2+}$/HEC (5cm, 25%)), eluent (1/1 (v/v) methanol/dichloromethane), flow rate (0.1 mLmin-1), wavelength (270 nm).

#4; [Ir(dfppy)$_2$(ppy)]



Elution conditions: column (Δ-[Ru(phen)$_3$]$^{2+}$/HEC (1cm, 2%)), eluent (acetonitrile), flow rate (0.1 mLmin-1), wavelength (300 nm).

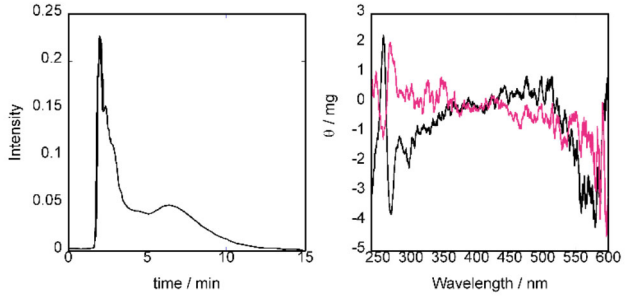
5: [Ir(piq)$_2$(ppy)]



Elution conditions: column (Δ-[Ru(phen)$_3$]$^{2+}$/HEC (1cm, 2%)), eluent (acetonitrile), flow rate (0.1 mLmin^{-1}), wavelength (400 nm).

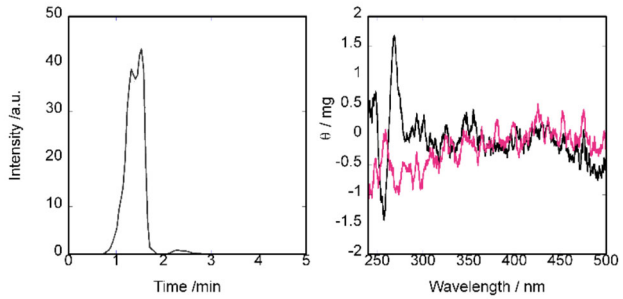
Conditions: column (5cm, 2%), eluent (acetonitrile), flow rate (0.1 mLmin^{-1}), wavelength (400 nm).

6 *trans*-[Ir(^{i}PrBQ)$_2$(dbm)]



Elution conditions: column (Δ-[Ru(phen)$_3$]$^{2+}$/HEC (5cm, 100%)), eluent (2/1 (v/v) methanol/dichloromethane), flow rate (0.1 mLmin^{-1}), wavelength (300 nm).

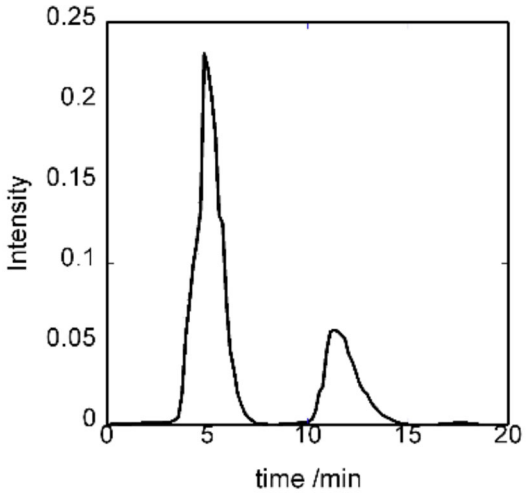
7: *trans*-[Ir(^{i}PrBQ)$_2$(heptacac)]



Elution conditions: column (Δ-[Ru(phen)$_3$]$^{2+}$/HEC (5cm, 100%)), eluent (2/1 (v/v) methanol/dichloromethane), flow rate (0.1 mLmin^{-1}), wavelength (300 nm).

5. Analyses of optical purity of eluted [Ir(ppy)$_2$(dmbpy)]$^+$ by use of a chiral column

The optical purity of partially resolved [Ir(ppy)$_2$(dmbpy)]$^+$ was analyzed by eluting the collected fraction of the complex through a commercial HPLC column (4mm (i.d.) x 25cm) (Chiral Pack IA, Daicel Ind. Co. (Japan)). From the areas of the first and second bands, the injected solution was concluded to contain Λ-[Ir(ppy)$_2$(dmbpy)]$^+$ at the optical purity of 60 %.



Elution conditions: column (Chiral Pack IA, Daicel Ind. Co. (Japan)). eluent (acetonitrile containing 1% (v/v) trifluoroacetic acid and 1% (v/v) diethyl amine), flow rate (0.5 mLmin-1), wavelength (270 nm). The first and second peaks corresponded to Δ- and Λ-enantiomers, respectively.

6. Vibrational circular dichroism for *cis*-[Ir(bzq)$_2$(PBO)]

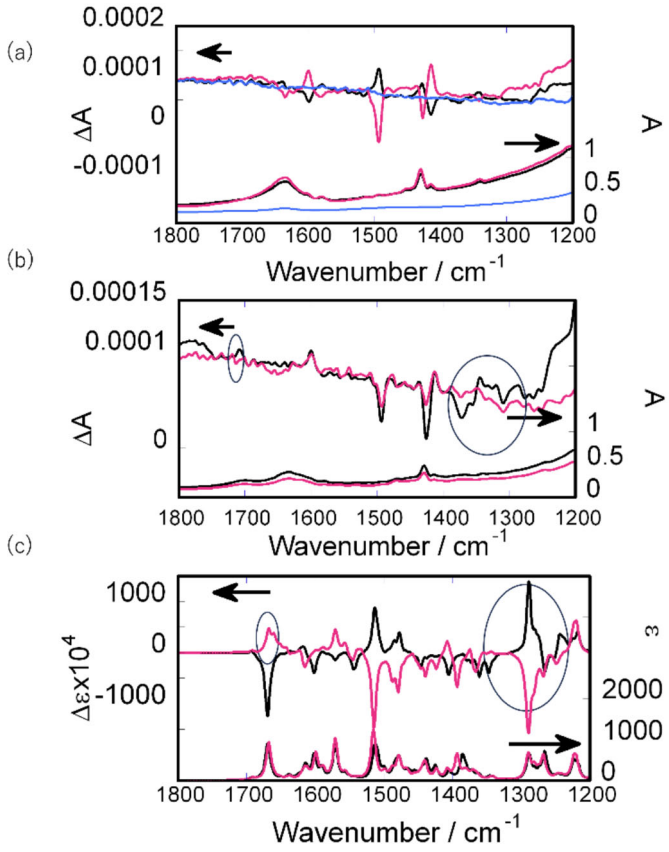


Figure S4. (a)The experimental VCD spectra of montmorillonite (Na-Mt) samples containing Λ- or Δ-[Ru(phen)$_3$]$^{2+}$ (denoted as Λ- or Δ-[Ru(phen)$_3$]$^{2+}$/Mt, respectively). Black, red and blue curves are for Λ-[Ru(phen)$_3$]$^{2+}$/Mt, Δ-[Ru(phen)$_3$]$^{2+}$/Mt and Na-Mt, respectively.

(b) The experimental VCD spectra of montmorillonite samples containing a pair of Λ-*cis*-[Ir(bzq)$_2$(PBO)]/Δ-[Ru(phen)$_3$]$^{2+}$ or Δ-*cis*-[Ir(bzq)$_2$(PBO)]/Δ-[Ru(phen)$_3$]$^{2+}$; The black and red lines are Λ-*cis*-[Ir(bzq)$_2$(PBO)]/Δ-[Ru(phen)$_3$]$^{2+}$/Mt (the quasi-racemic pair), Δ-*cis*-[Ir(bzq)$_2$(PBO)]/Δ-[Ru(phen)$_3$]$^{2+}$/Mt (quasi-enantiomeric pair), respectively. The circles show effect of quasi-enantiomeric (Δ-Δ) or quasi- racemic pair (Λ-Δ) of VCD spectra.

(c) The calculated VCD spectra using the optimized association structures. The black and red lines are Λ-*cis*-[Ir(bzq)$_2$(PBO)]/ Δ-[Ru(phen)$_3$]$^{2+}$/Mt (the quasi-racemic pair), Δ-*cis*-[Ir(bzq)$_2$(PBO)]/ Δ-[Ru(phen)$_3$]$^{2+}$/Mt (quasi-enantiomeric pair), respectively.